

Updated scalar sector constraints in Higgs triplet model

Dipankar Das¹, Arcadi Santamaria²

*Departament de Física Tèorica, Universitat de València and IFIC, Universitat de València-CSIC
Dr. Moliner 50, E-46100 Burjassot (València), Spain*

Abstract

We show that in the Higgs triplet model, after the Higgs discovery, the mixing angle in the CP-even sector can be strongly constrained from unitarity. We also discuss how large quantum effects in $h \rightarrow \gamma\gamma$ may arise in a SM-like scenario and a certain part of the parameter space can be ruled out from the diphoton signal strength. Using T -parameter and diphoton signal strength measurements, we update the bounds on the nonstandard scalar masses.

1 Introduction

Neutrino masses are one of the main motivations we have at present for physics beyond the Standard Model (SM). Although a minimal extension of the SM by adding three right-handed neutrinos with Dirac mass terms is still allowed by all neutrino data, this is not the preferred scenario for it does not explain the smallness of neutrino masses or why lepton number should exactly be conserved.

Scenarios in which the smallness of neutrino masses is linked to the non-conservation of lepton number are usually considered more natural. The simplest versions of these scenarios are realized at tree level and are known under the name of the seesaw mechanisms. Seesaws of type I [1–5] and III [6, 7] extend the SM with new fermions, singlet and triplet respectively, with a Majorana mass term, M , which breaks explicitly lepton number. On the other hand, seesaw of type II [8–12] adds only a scalar triplet with hypercharge 2. In this case, lepton number is broken explicitly in the scalar potential by a trilinear coupling, μ (see also [13, 14] for a variation with lepton number broken spontaneously).

Seesaws of type I and III give neutrino masses of order $m_\nu \sim yv_d^2/M$ with y being the Yukawa coupling and v_d the vacuum expectation value (VEV) of the SM doublet. Then, if $M \gg v_d$, masses can naturally be small. However, the same parameters that appear in the neutrino masses also appear in the mixing of new fermions with ordinary fermions, which is proportional to yv_d/M and must be very small. This makes these types of models very difficult to test.

Seesaw of type II, however, generates neutrino masses of order $m_\nu \sim y\mu v_d^2/M^2$, where now y is the Yukawa coupling of the scalar triplet to lepton doublets and M the triplet mass. The trilinear coupling μ is protected by symmetry and can be naturally small. This allows for small neutrino masses compatible with a rich phenomenology (the new scalars of the model could be produced at the LHC [15–22] and there could be lepton flavor violating processes like $\mu \rightarrow 3e$ or $\mu \rightarrow e\gamma$ [23–27]), raising the possibility to test the mechanism of neutrino masses in non-oscillation experiments.

¹dipankar.das@uv.es

²arcadi.santamaria@uv.es

In an effort to fixate the scalar spectrum of the model, in this article we revisit the scalar potential of the type II seesaw model taking into account unitarity and the stability of the potential. Moreover, on the phenomenological side, we will also consider the constraints coming from the oblique T -parameter and Higgs decay branching ratios, in particular $h \rightarrow \gamma\gamma$, which are largely independent on the other sectors of the theory (Yukawa couplings and neutrino masses). In fact, the one-loop T -parameter only depends, to a good approximation, on the mass splitting between the scalars, while the new contributions to $h \rightarrow \gamma\gamma$ can be expressed in terms of the scalar masses and the mixing angle in the neutral scalar sector.

A very important ingredient of our analysis is the requirement that the triplet scalar VEV, v_t , is much smaller than the electroweak scale. This is, in part, required by the tree-level ρ -parameter and in part, by the requirement of small neutrino masses. It has been noticed, in this case, that the some relations involving the scalar masses can be obtained and that the T -parameter constrains the splitting to be less than about 50 GeV (see for instance [18]). We will re-derive these constraints by using perturbative unitarity and the T -parameter. After this, the spectrum of scalar masses is practically fixed up to a global scale and a small splitting between masses and can be expressed in terms of three parameters (apart from the known parameters, the Higgs mass and the electroweak scale, and the triplet VEV which becomes irrelevant for $v_t < 1$ GeV). Then, we will derive a lower bound on the global scale by adding present data on $h \rightarrow \gamma\gamma$.

Similar analyses have been performed several times in the literature [28–31]. But we differ from those in the sense that we express our results in terms of the experimentally measurable quantities. In the process, we have been able to unravel some features which, we believe, have not been emphasized before. Additionally we also point out that the current measurement of the diphoton signal strength enables us to put lower limits on the nonstandard scalar masses, which are competitive or, in some cases, better than the direct search limits.

In Section 2 we study the scalar potential, the scalar mass spectrum and the constraints from unitarity and stability. In Section 3 we perform a complete numerical analysis by including also the constraints from the ρ -parameter. In Section 4 we study the impact of the data on $h \rightarrow \gamma\gamma$ and obtain the lower bound on the masses. Finally in Section 5 we present our conclusions.

2 The scalar potential

The Type II seesaw model extends the Higgs sector of the standard model by adding one scalar $SU(2)_L$ triplet (Δ) with hypercharge, $Y_\Delta = 2$. The most general scalar potential involving this triplet and the standard $SU(2)_L$ doublet, Φ , is given by [28]

$$V = -m_\Phi^2 (\Phi^\dagger \Phi) + M^2 \text{Tr} (\Delta^\dagger \Delta) + \{\mu (\Phi^T i\sigma_2 \Delta^\dagger \Phi) + \text{h.c.}\} + \frac{\lambda}{4} (\Phi^\dagger \Phi)^2 + \lambda_1 (\Phi^\dagger \Phi) \text{Tr} (\Delta^\dagger \Delta) + \lambda_2 \{\text{Tr} (\Delta^\dagger \Delta)\}^2 + \lambda_3 \text{Tr} [(\Delta^\dagger \Delta)^2] + \lambda_4 (\Phi^\dagger \Delta \Delta^\dagger \Phi), \quad (1)$$

where ‘Tr’ represents the trace over 2×2 matrices and σ_2 is the second Pauli matrix. We can take all the parameters in the potential to be real without any loss of generality [32, 33]. Denoting by v_d (v_t) the VEV of the doublet (triplet) scalar field, the minimization conditions read

$$m_\Phi^2 = \frac{\lambda v_d^2}{4} + \frac{(\lambda_1 + \lambda_4)v_t^2}{2} - \sqrt{2}\mu v_t, \quad (2a)$$

$$M^2 = -(\lambda_2 + \lambda_3)v_t^2 - \frac{(\lambda_1 + \lambda_4)v_d^2}{2} + \frac{\mu v_d^2}{\sqrt{2}v_t}. \quad (2b)$$

After the spontaneous symmetry breaking, we represent the scalar multiplets in the following way:

$$\Phi = \frac{1}{\sqrt{2}} \begin{pmatrix} \sqrt{2}w_d^+ \\ v_d + h_d + iz_d \end{pmatrix}, \quad \Delta = \frac{1}{\sqrt{2}} \begin{pmatrix} w_t^+ & \sqrt{2}\delta^{++} \\ v_t + h_t + iz_t & -w_t^+ \end{pmatrix}, \quad (3)$$

and the electroweak VEV is then given by,

$$v = \sqrt{v_d^2 + 2v_t^2} = 246 \text{ GeV}. \quad (4)$$

From the observed value of the electroweak ρ -parameter, v_t is expected to be $\mathcal{O}(1 \text{ GeV})$ or less [14,17,18,28,34].

2.1 Physical eigenstates

Using Eq. (2) we first trade m_{Φ}^2 and M^2 for v_d and v_t in the potential of Eq. (1). The fields, $\delta^{\pm\pm}$, represent the doubly charged scalar with mass

$$m_{++}^2 = \frac{\mu v_d^2}{\sqrt{2}v_t} - \frac{\lambda_4}{2}v_d^2 - \lambda_3v_t^2. \quad (5)$$

The mass squared matrix in the singly charged sector can be rotated to the physical basis through

$$\begin{pmatrix} \omega^\pm \\ H^\pm \end{pmatrix} = \begin{pmatrix} \cos \beta & \sin \beta \\ -\sin \beta & \cos \beta \end{pmatrix} \begin{pmatrix} w_d^\pm \\ w_t^\pm \end{pmatrix}, \quad \text{with } \tan \beta = \frac{\sqrt{2}v_t}{v_d}, \quad (6)$$

to obtain the charged Goldstone (ω^\pm) along with a singly charged scalar (H^\pm) with mass

$$m_+^2 = \frac{(2\sqrt{2}\mu - \lambda_4v_t)}{4v_t}(v_d^2 + 2v_t^2). \quad (7)$$

The assumption of real VEVs allows us to define electrically neutral mass eigenstates which are also eigenstates of CP . The mass squared matrix in the CP -odd sector can be rotated to the physical basis through

$$\begin{pmatrix} \zeta \\ A \end{pmatrix} = \begin{pmatrix} \cos \beta' & \sin \beta' \\ -\sin \beta' & \cos \beta' \end{pmatrix} \begin{pmatrix} z_d \\ z_t \end{pmatrix}, \quad \text{with } \tan \beta' = \frac{2v_t}{v_d}, \quad (8)$$

to obtain the neutral Goldstone (ζ) along with a pseudoscalar (A) with mass

$$m_A^2 = \frac{\mu}{\sqrt{2}v_t}(v_d^2 + 4v_t^2). \quad (9)$$

Finally, for the CP -even part we have:

$$M_S^2 = \begin{pmatrix} A_S & -B_S \\ -B_S & C_S \end{pmatrix}, \quad (10a)$$

$$\text{where, } A_S = \frac{\lambda v_d^2}{2}, \quad (10b)$$

$$B_S = \sqrt{2}\mu v_d - (\lambda_1 + \lambda_4)v_t v_d, \quad (10c)$$

$$C_S = \frac{\mu v_d^2}{\sqrt{2}v_t} + 2(\lambda_2 + \lambda_3)v_t^2. \quad (10d)$$

We can obtain the physical eigenstates through the following rotation:

$$\begin{pmatrix} h \\ H \end{pmatrix} = \begin{pmatrix} \cos \alpha & \sin \alpha \\ -\sin \alpha & \cos \alpha \end{pmatrix} \begin{pmatrix} h_d \\ h_t \end{pmatrix}, \quad \text{with, } \tan 2\alpha = \frac{2B_S}{C_S - A_S} = \frac{\sqrt{2}\mu v_d - (\lambda_1 + \lambda_4)v_t v_d}{\frac{\mu v_d^2}{2\sqrt{2}v_t} + (\lambda_2 + \lambda_3)v_t^2 - \frac{\lambda v_d^2}{4}}, \quad (11a)$$

$$\text{with masses, } m_h^2 = (A_S + C_S) - \sqrt{(A_S - C_S)^2 + 4B_S^2}, \quad (11b)$$

$$m_H^2 = (A_S + C_S) + \sqrt{(A_S - C_S)^2 + 4B_S^2}. \quad (11c)$$

SM like limit: Even with $v_t \ll v_d$, to make the tree level couplings of the lightest CP -even scalar (h) close to those in the SM, we need to set $\sin \alpha = 0$. From Eq. (11a) we see that there are two different ways to obtain this limit as discussed below:

Case I: The first option is to invoke a fine tuning so that the numerator in the expression for $\tan 2\alpha$ vanishes. The condition reads:

$$\sqrt{2}\mu = (\lambda_1 + \lambda_4)v_t, \quad (12a)$$

$$\Rightarrow \sin \alpha = 0, \quad \text{with } v_t \neq 0. \quad (12b)$$

Note that, in this case, we can make the tree level couplings of h to be close to SM *without* demanding v_t to be exactly zero. This limit is interesting in view of the fact that we can still have small neutrino masses through a small value for v_t and at the same time be very close to the SM. But later we will show that the charged scalars, in this limit, can contribute substantially in the diphoton decay amplitude and therefore this limit is *ruled out*.

Case II: In a second and more conventional approach, the SM-like limit is obtained as a direct consequence of v_t being arbitrarily small. To be more precise, in the limit and $M^2 \gg v^2$, we can approximate Eq. (2b) as

$$v_t \approx \frac{\mu v^2}{\sqrt{2}M^2}. \quad (13)$$

In this case the expression for $\tan 2\alpha$ in Eq. (11a) can be simplified into

$$\tan 2\alpha \approx \frac{4v_t}{v_d}, \quad \Rightarrow \sin \alpha \approx \frac{2v_t}{v_d}, \quad \text{with } v_t \rightarrow 0. \quad (14)$$

As we will show later, this limit corresponds to the decoupling of heavy nonstandard scalars.

It is now instructive to count the number of free parameters in the scalar potential. Note that, Eq. (1) contains eight free parameters. As mentioned before, m_{Φ}^2 and M^2 can be traded in favor of v_d and v_t . The remaining six parameters can be exchanged for five physical masses and the mixing angle, α , as follows [28]:

$$\mu = \frac{\sqrt{2}m_A^2 v_t}{v_d^2 + 4v_t^2}, \quad (15a)$$

$$\lambda = \frac{2}{v_d^2} (m_H^2 \sin^2 \alpha + m_h^2 \cos^2 \alpha), \quad (15b)$$

$$\lambda_1 = \frac{4m_+^2}{v_d^2 + 2v_t^2} - \frac{2m_A^2}{v_d^2 + 4v_t^2} - \frac{\sin \alpha \cos \alpha}{v_d v_t} (m_H^2 - m_h^2), \quad (15c)$$

$$\lambda_2 = \frac{1}{v_t^2} \left[\frac{1}{2} (m_h^2 \sin^2 \alpha + m_H^2 \cos^2 \alpha) + \frac{v_d^2 m_A^2}{2(v_d^2 + 4v_t^2)} - \frac{2v_d^2 m_+^2}{v_d^2 + 2v_t^2} + m_{++}^2 \right], \quad (15d)$$

$$\lambda_3 = \frac{1}{v_t^2} \left[\frac{2v_d^2 m_+^2}{v_d^2 + 2v_t^2} - \frac{v_d^2 m_A^2}{v_d^2 + 4v_t^2} - m_{++}^2 \right], \quad (15e)$$

$$\lambda_4 = \frac{4m_A^2}{v_d^2 + 4v_t^2} - \frac{4m_+^2}{v_d^2 + 2v_t^2}. \quad (15f)$$

Among the eight redefined parameters that appear on the RHS of Eq. (15), not all are unknown. We already know $v = \sqrt{v_d^2 + 2v_t^2} = 246$ GeV and under the assumption that the lightest CP -even Higgs is what has been found at the LHC, $m_h \approx 125$ GeV is also known. The compatibility of Higgs signal strengths into different decay channels with their corresponding SM expectations tells us to focus near the SM-like limit, $\sin \alpha \approx 0$. We will see how the smallness of v_t in association with unitarity and stability entail strong correlations among the remaining four nonstandard masses, $\{m_H, m_A, m_+, m_{++}\}$, making the scalar potential of Type II seesaw model constrained very strongly.

2.2 Theoretical constraints from vacuum stability and unitarity

We need to ensure that there is no direction in the field space along which the potential becomes infinitely negative. The conditions for the potential of Eq. (1) to be bounded from below read [35]

$$\lambda \geq 0, \quad \lambda_2 + \lambda_3 \geq 0, \quad \lambda_2 + \frac{\lambda_3}{2} \geq 0, \quad \lambda_1 + \sqrt{\lambda(\lambda_2 + \lambda_3)} \geq 0, \quad \lambda_1 + \lambda_4 + \sqrt{\lambda(\lambda_2 + \lambda_3)} \geq 0, \quad (16a)$$

$$\text{and,} \quad \left[|\lambda_4| \sqrt{\lambda_2 + \lambda_3} - \lambda_3 \sqrt{\lambda} \geq 0, \quad \text{or,} \quad 2\lambda_1 + \lambda_4 + \sqrt{(2\lambda\lambda_3 - \lambda_4^2) \left(\frac{2\lambda_2}{\lambda_3} + 1 \right)} \geq 0 \right]. \quad (16b)$$

The S -matrix eigenvalues that will be constrained from unitarity of the scattering amplitudes are also listed below [28]:

$$\left| (\lambda + 4\lambda_2 + 8\lambda_3) \pm \sqrt{(\lambda - 4\lambda_2 - 8\lambda_3)^2 + 16\lambda_4^2} \right| \leq 64\pi, \quad (17a)$$

$$\left| (3\lambda + 16\lambda_2 + 12\lambda_3) \pm \sqrt{(3\lambda - 16\lambda_2 - 12\lambda_3)^2 + 24(2\lambda_1 + \lambda_4)^2} \right| \leq 64\pi, \quad (17b)$$

$$|\lambda| \leq 32\pi, \quad (17c)$$

$$|2\lambda_1 + 3\lambda_4| \leq 32\pi, \quad (17d)$$

$$|2\lambda_1 - \lambda_4| \leq 32\pi, \quad (17e)$$

$$|\lambda_1| \leq 16\pi, \quad (17f)$$

$$|\lambda_1 + \lambda_4| \leq 16\pi, \quad (17g)$$

$$|2\lambda_2 - \lambda_3| \leq 16\pi, \quad (17h)$$

$$|\lambda_2| \leq 8\pi, \quad (17i)$$

$$|\lambda_2 + \lambda_3| \leq 8\pi. \quad (17j)$$

3 Numerical analysis and results

As a first level of simplification, we can use Eq. (15) into the inequality (17j) and remembering $\lambda_2 + \lambda_3 \geq 0$, we may write

$$0 \leq (m_h^2 \sin^2 \alpha + m_H^2 \cos^2 \alpha) - \frac{v_d^2 m_A^2}{v_d^2 + 4v_t^2} \leq 16\pi v_t^2. \quad (18)$$

Therefore, for $v_t < \mathcal{O}(1 \text{ GeV})$, we can very well approximate

$$m_A^2 \approx m_h^2 \sin^2 \alpha + m_H^2 \cos^2 \alpha. \quad (19)$$

This automatically implies $m_h < m_A < m_H$. Similar considerations for the inequalities (17h) or (17i) enable us to express the doubly charged scalar mass as follows:

$$m_{++}^2 \approx 2m_+^2 - m_A^2 \approx 2m_+^2 - (m_h^2 \sin^2 \alpha + m_H^2 \cos^2 \alpha). \quad (20)$$

We will exemplify our numerical results by setting $v_t = 1 \text{ GeV}$. We also take $v = 246 \text{ GeV}$ and $m_h = 125 \text{ GeV}$ as input parameters. Then we perform random scan over the $\{\sin \alpha, m_H, m_+\}$ space by varying the parameters within the following ranges:

$$\sin \alpha \in [-0.2, 0.2], \quad m_H \in [125, 2000] \text{ GeV}, \quad m_+ \in [0, 2000] \text{ GeV}, \quad (21)$$

and calculate m_A and m_{++} through the relations (19) and (20)³. In anticipation that the Higgs data will continue to agree with the SM with increasing accuracy in the upcoming runs of the LHC, we vary $\sin \alpha$ in a

³Nonzero values of λ_2 and λ_3 will cause negligible deviations from Eqs. (19) and (20). We have taken this effect into account in our numerical analysis.

rather narrow range around $\sin \alpha = 0$. Next we compute the λ_i s using Eq. (15) and check whether the unitarity and stability conditions, given in Eqs. (17) and (16), are satisfied. Note that, since we are scanning in terms of the physical parameters, positivity of the masses are guaranteed and therefore, we are in a local minimum. Moreover, we have explicitly checked that $V_{\min} < 0$ for every point in our scan. We discuss below the results of our analysis.

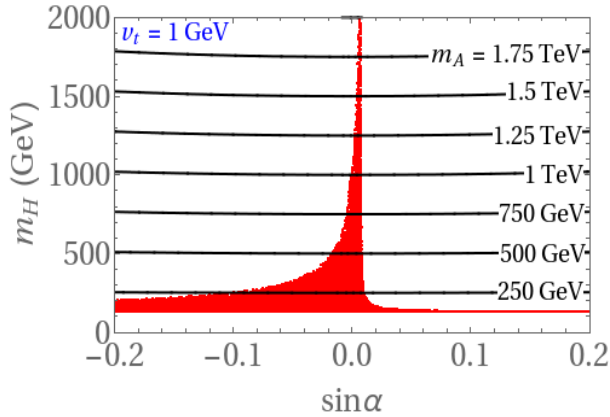


Figure 1: Allowed points in $\sin \alpha$ - m_H plane from unitarity and stability for $v_t = 1$ GeV. The continuous lines are contours for m_A drawn using Eq. (19).

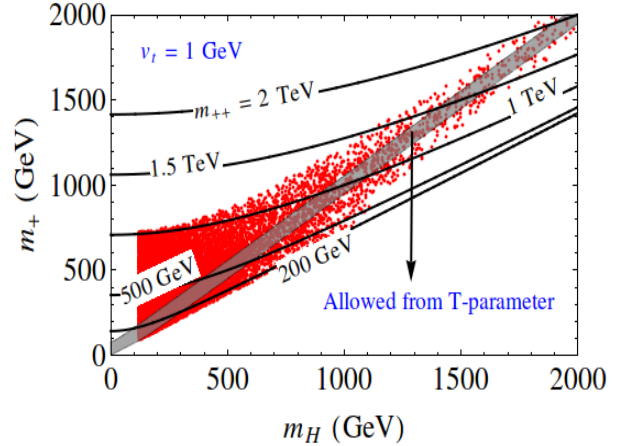


Figure 2: Allowed points in m_H - m_+ plane from unitarity and stability for $v_t = 1$ GeV. The continuous lines are contours for m_{++} drawn using Eq. (20) for $\sin \alpha \approx 0$. The allowed region from T-parameter has also been shaded assuming $m_H \approx m_A$.

From Fig. 1 we see that a heavy m_H requires $\sin \alpha \approx 0$, *i.e.*, we are automatically pushed towards a SM-like situation for small v_t and heavy nonstandard scalars. However a closer inspection of Fig. 1 reveals that the peak does not occur precisely at $\sin \alpha = 0$ but at a small non negative value of $\sin \alpha$. The reason for this can be understood from the unitarity condition (17g) which, in terms of the physical masses reads

$$\left| m_h^2 \sin^2 \alpha + m_H^2 \cos^2 \alpha - \sin \alpha \cos \alpha \frac{v_d}{2v_t} (m_H^2 - m_h^2) \right| \leq 8\pi v_d^2, \quad (22)$$

where, we have used Eq. (19) to substitute for m_A . One interesting thing to note from above inequality is that, when $v_t \neq 0$, the value of m_H is bounded from above in the SM-like limit, $\sin \alpha = 0$. But what is more interesting is to find that, for large m_H and small $\sin \alpha$, the expression on the LHS of (22) vanishes for $\sin \alpha \approx 2v_t/v_d$ and so the inequality is trivially satisfied. Thus the location of the peak on the horizontal axis of Fig. 1 is a direct reflection of a small value of v_t . Smaller the value for v_t , closer is the peak to $\sin \alpha = 0$.

Strictly speaking, the peak in Fig. 1 does not extend up to infinity along the vertical axis. This is because the unitarity condition (17c) which in terms of physical masses reads

$$(m_H^2 \sin^2 \alpha + m_h^2 \cos^2 \alpha) \leq 16\pi v_d^2, \quad (23)$$

always puts an upper bound on m_H for nonzero $\sin \alpha$. But for $v_t \rightarrow 0$ the peak of Fig. 1 at $\sin \alpha = 0$ which corresponds to the decoupling limit as defined in Eq. (14) and in this case, the bound from (22) can be alleviated and infinitely heavy nonstandard scalars can be allowed.

Fig. 2 depicts that the splitting between m_H and m_+ can be restricted from unitarity and stability. In Figs. 1 and 2 we have also drawn the contours of m_A and m_{++} to emphasize that due to the correlation between different parameters, experimental bound on any of the nonstandard masses can be translated into indirect bounds on the other masses too. To illustrate, if we can rule out a doubly charged scalar below 500 GeV from

direct searches at the LHC, then, from Fig. 2, we also forbid a singly charged scalar below 350 GeV. Note that, these correlated bounds do not crucially depend on the numerical value of v_t as long as it is small. In passing we also remark that although the contours of m_{++} in Fig. 2 have been drawn for $\sin \alpha = 0$, they are not appreciably modified for $|\sin \alpha| < 0.2$.

Things become more interesting when we superimpose, in Fig. 2, the constraint arising from the electroweak T -parameter. For $v_t = 1$ GeV or less, the major contribution to the T -parameter comes from the loops involving the new nonstandard scalars. With $\sin \alpha \approx 0$ and $m_H \approx m_A$ (these two approximations can already be justified from Fig. 1), the new physics contribution to the electroweak T -parameter is given by [29, 36]

$$\Delta T = \frac{1}{4\pi \sin^2 \theta_w m_W^2} [F(m_+^2, m_A^2) + F(m_{++}^2, m_+^2)] , \quad (24)$$

where, θ_w and m_W are the Weinberg angle and the W -boson mass respectively, and

$$F(x, y) = \frac{x+y}{2} - \frac{xy}{x-y} \ln \left(\frac{x}{y} \right) . \quad (25)$$

In Eq. (24) we further use the relation (20) to substitute for m_{++} . Taking the new physics contribution to the T -parameter as [37]

$$\Delta T < 0.2 \text{ at } 95\% \text{C.L.} , \quad (26)$$

we draw the allowed region in Fig. 2. From there we see that the combined constraint implies that all the nonstandard scalars should be nearly degenerate. Using the correlation of Eq. (20), and denoting the typical mass difference, $(m_+ - m_{++})$ by δ ($\delta \ll m$), we can simplify the expression of the T -parameter as follows:

$$\Delta T \approx \frac{\delta^2}{3\pi \sin^2 \theta_w m_W^2} . \quad (27)$$

Using the experimental number we can then find $|\delta| \lesssim 50$ GeV.

4 Impact on loop induced Higgs decays

Since the quarks couple only with the doublet and the physical scalar, h , in general, is a mixed state of doublet and triplet fields, the tree level couplings of h will be modified from those in the SM. We define a generic modification factor for the fermions and vector bosons as follows:

$$\kappa_X = \frac{g_{hXX}^{\text{model}}}{g_{hXX}^{\text{SM}}} . \quad (28)$$

Then, for $v_t \ll v_d$, one can easily calculate [28]

$$\kappa_q \approx \kappa_V \approx \cos \alpha , \quad (29)$$

where, q represents any fermion and $V = W, Z$. Denoting by f_X the percentage of h produced via the channel X , we can express the modification of the Higgs production cross section as follows:

$$\mathcal{R}_P = \frac{\sigma(pp \rightarrow h)^{\text{model}}}{\sigma(pp \rightarrow h)^{\text{SM}}} = \kappa_q^2 (f_{ggF} + f_{tth}) + \kappa_V^2 (f_{VBF} + f_{Vh}) , \quad (30)$$

where, $f_{ggF} \approx 87.5\%$, $f_{VBF} \approx 7\%$, $f_{Vh} \approx 5\%$ and $f_{tth} \approx 0.5\%$ at a CM energy of 7 and 8 TeV [37]. We know that a 125 GeV SM Higgs decays into VV^* channel with nearly 24% branching ratio and the rest decays almost

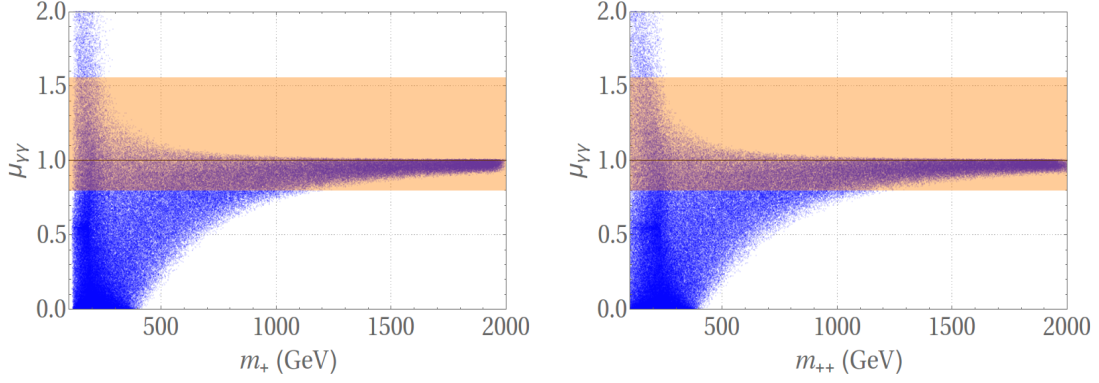


Figure 3: Dependence of the diphoton signal strength on m_+ and m_{++} plotted for the points that survive from the constraints of unitarity, stability and T -parameter (blue points) for $v_t = 1$ GeV. The horizontal band represents the 2σ experimental limit from the combined fit of ATLAS and CMS results [38].

entirely into two-body fermionic channels and into two gluons. Thus the modification of the total decay width can be expressed as

$$\mathcal{R} = \frac{\Gamma^{\text{model}}}{\Gamma^{\text{SM}}} = \kappa_q^2 \cdot 76\% + \kappa_V^2 \cdot 24\%. \quad (31)$$

Now we turn our attention to the modification of the partial decay widths of loop induced Higgs decays like $h \rightarrow \gamma\gamma$. To display conveniently the contribution of the charged scalar loops to the decay amplitude, we define dimensionless parameters κ_+ and κ_{++} in the following way,

$$\kappa_+ = \frac{m_W}{gm_+^2} g_{hH^+H^-}, \quad (32a)$$

$$\kappa_{++} = \frac{m_W}{gm_{++}^2} g_{h\delta^{++}\delta^{--}}, \quad (32b)$$

where, the general expressions for $g_{hH^+H^-}$ and $g_{h\delta^{++}\delta^{--}}$ are given by

$$g_{hH^+H^-} = -\frac{A_+ \cos \alpha + B_+ \sin \alpha}{v_t v_d (v_d^2 + 2v_t^2)(v_d^2 + 4v_t^2)}, \quad (33a)$$

$$\text{with, } A_+ = 2v_t(v_d^2 + 4v_t^2)(m_+^2 v_d^2 + m_h^2 v_t^2), \quad (33b)$$

$$B_+ = v_d \{ (v_d^2 + 4v_t^2)(m_h^2 v_d^2 + 4m_+^2 v_t^2) - m_A^2 (v_d^2 + 2v_t^2)^2 \}, \quad (33c)$$

$$\text{and, } g_{h\delta^{++}\delta^{--}} = -\frac{A_{++} \cos \alpha + B_{++} \sin \alpha}{v_t (v_d^2 + 2v_t^2)(v_d^2 + 4v_t^2)}, \quad (33d)$$

$$\text{with, } A_{++} = 2v_t v_d \{ 2m_+^2 (v_d^2 + 4v_t^2) - m_A^2 (v_d^2 + 2v_t^2) \}, \quad (33e)$$

$$B_{++} = [m_A^2 v_d^2 (v_d^2 + 2v_t^2) - (v_d^2 + 4v_t^2) \{ 4m_+^2 - (2m_{++}^2 + m_h^2)(v_d^2 + 2v_t^2) \}]. \quad (33f)$$

With these, the modification of the diphoton decay width can be written as

$$\mathcal{R}_{\gamma\gamma} = \frac{\Gamma(h \rightarrow \gamma\gamma)^{\text{model}}}{\Gamma(h \rightarrow \gamma\gamma)^{\text{SM}}} = \frac{|\kappa_V \mathcal{F}_1(\tau_W) + \frac{4}{3} \kappa_q \mathcal{F}_{1/2}(\tau_t) + \kappa_+ \mathcal{F}_0(\tau_+) + 4\kappa_{++} \mathcal{F}_0(\tau_{++})|^2}{|\mathcal{F}_1(\tau_W) + \frac{4}{3} \mathcal{F}_{1/2}(\tau_t)|^2}, \quad (34)$$

where, using the notation, $\tau_x \equiv (2m_x/m_h)^2$, the \mathcal{F} functions can be written as [39]

$$\mathcal{F}_1(\tau_x) = 2 + 3\tau_x + 3\tau_x(2 - \tau_x)\mathcal{G}(\tau_x), \quad (35a)$$

$$\mathcal{F}_{1/2}(\tau_x) = -2\tau_x \{ 1 + (1 - \tau_x)\mathcal{G}(\tau_x) \}, \quad (35b)$$

$$\mathcal{F}_0(\tau_x) = -\tau_x \{1 - \tau_x \mathcal{G}(\tau_x)\}, \quad (35c)$$

$$\text{with, } \mathcal{G}(\tau) = \begin{cases} \left[\sin^{-1} \left(\sqrt{\frac{1}{\tau}} \right) \right]^2, & \text{for } \tau \geq 1, \\ -\frac{1}{4} \left[\ln \left(\frac{1+\sqrt{1-\tau}}{1-\sqrt{1-\tau}} \right) - i\pi \right]^2, & \text{for } \tau < 1. \end{cases} \quad (35d)$$

Now we can write the modified Higgs signal strength as follows:

$$\mu_{\gamma\gamma} = \frac{\mathcal{R}_P}{\mathcal{R}} \times \mathcal{R}_{\gamma\gamma}. \quad (36)$$

In Fig. 3 we have shown how $\mu_{\gamma\gamma}$ behaves with the charged scalar masses. Here, one should note that the signal strength is suppressed compared to the SM expectations for heavy charged scalars. Thus observation of an excess in the diphoton channel, in future runs of the LHC, will disfavor the possibility of heavy charged scalars in this model. In passing, we comment that although we have assumed $v_t = 1$ GeV in Fig. 3, the above conclusions do not crucially depend on our numerical choice of v_t as long as it remains small.

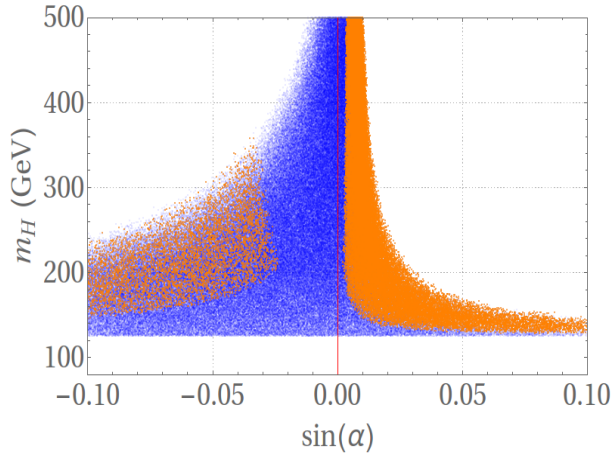


Figure 4: The blue points (in the background) are allowed from unitarity, stability and T -parameter for $v_t = 1$ GeV. The yellow points are those which survive when 2σ constraint from $\mu_{\gamma\gamma}$ are added on top of it. Clearly, a narrow band around $\sin \alpha \approx 0$ can be ruled out from $\mu_{\gamma\gamma}$.

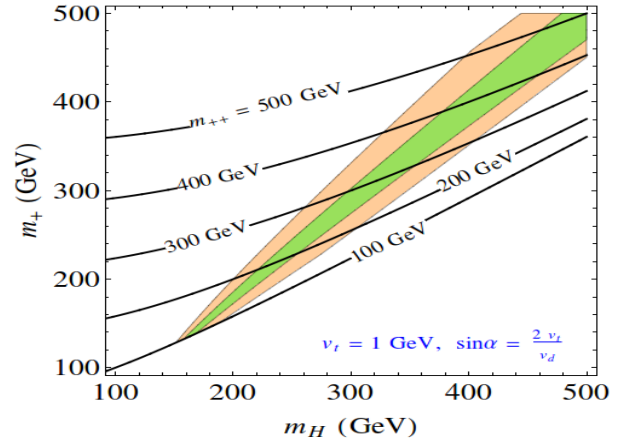


Figure 5: The outer orange region is allowed from T -parameter and the observed diphoton signal strength at 95% CL. The inner green region represents how the constraint will tighten if $\mu_{\gamma\gamma}$ is measured to be $1 \pm 5\%$. Contours of m_{++} are also shown.

Next, we can also define, similar to Eq. (36), the modified signal strength for the $h \rightarrow Z\gamma$ decay channel, $\mu_{Z\gamma}$. However, for brevity, we do not display the explicit expressions here. Interested readers can find the relevant formulas in some earlier papers [30, 31, 40, 41]. As has been noted in these references, since the sign of the $H^+H^-Z\gamma$ vertex is opposite to that of the $\delta^{++}\delta^{--}Z\gamma$ vertex, the singly charged scalar loop interfere destructively with the doubly charged one in the $h \rightarrow Z\gamma$ amplitude. Consequently, in some region of the parameter space depending on which loop dominates, we can have an *anti-correlation* between $\mu_{\gamma\gamma}$ and $\mu_{Z\gamma}$, *i.e.*, one is enhanced compared to the SM while the other is suppressed.

But the new thing that we want to add to this context is the understanding of the behavior of $\mu_{\gamma\gamma}$ and $\mu_{Z\gamma}$ in the SM-like scenario. One should note that, as the charged scalars become heavy, the function $\mathcal{F}_0(\tau)$ in Eq. (35c) saturates to $1/3$. Hence the decoupling of the charged scalars from the loop induced Higgs decays depends on how κ_+ (κ_{++}) behaves with increasing m_+ (m_{++}). We can easily check that, in the SM-like case defined by Eq. (12b), the trilinear couplings in Eqs. (33a) and (33d) take the following forms:

$$g_{hH^+H^-} = -\frac{2(m_+^2 v_d^2 + m_h^2 v_t^2)}{v_d(v_d^2 + 2v_t^2)} \approx -\frac{2m_+^2}{v_d}, \quad (37a)$$

$$\text{and, } g_{h\delta^{++}\delta^{--}} = -2v_d \left[\frac{2m_+^2}{v_d^2 + 2v_t^2} - \frac{m_A^2}{v_d^2 + 4v_t^2} \right] \approx -\frac{2m_{++}^2}{v_d}, \quad (37b)$$

where, in the final step we have used Eqs. (19) and (20). Thus it follows from Eq. (32) that $\kappa_+, \kappa_{++} \rightarrow -1$ when $m_+, m_{++} \gg m_h$. Consequently the charged scalars contribute substantially to the diphoton or Z -photon decay amplitudes even when their masses lie in the TeV regime. In fact, one can check from Eq. (36) that $\mu_{\gamma\gamma} \approx \mathcal{R}_{\gamma\gamma} \lesssim 0.5$ when $\sin \alpha = 0$ for finite v_t . Therefore the SM-like limit defined by Eq. (12b) is already forbidden from the current combined fit value of the diphoton signal strength, $\mu_{\gamma\gamma} = 1.16_{-0.18}^{+0.20}$ [38]. This feature has been clearly depicted in Fig. 4 where we can see that the region around $\sin \alpha = 0$ is ruled out from the Higgs to diphoton data. The reason for this large quantum effect for heavy masses can be understood once we realize that both the VEVs in this case are nonzero. This means the charged scalars obtain their masses entirely from spontaneous symmetry breaking (SSB), which leads to large quantum effects as also has been noted in the multi doublet context [42].

But in the SM-like limit defined by Eq. (14) one can obtain

$$g_{hH^+H^-} = -\frac{2(m_+^2 - m_A^2) + 2m_h^2}{v}, \quad (38a)$$

$$\text{and, } g_{h\delta^{++}\delta^{--}} = -\frac{2(m_{++}^2 - m_A^2) + 2m_h^2}{v}. \quad (38b)$$

Here we can easily see that the charged scalars can be decoupled in the limit,

$$m_+ \approx m_{++} \approx m_A \gg m_h. \quad (39)$$

Let us investigate the above limit in some greater detail. Since $v_t \rightarrow 0$ in this case, the triplet remains inert and M^2 in Eq. (1) serves as a free mass squared parameter not connected to SSB. Using Eq. (13) to recover M^2 from v_t and then plugging it in Eq. (15a) we can see that for this type of scenario, $m_A^2 \approx M^2$. Thus the condition (39) essentially implies that the charged scalars obtain all their masses from a non-SSB origin, which, not surprisingly, lead to decoupling in the same way as in the inert doublet models [42].

From the combined region in Fig. 4, we see that the space for m_H (or, m_A) is severely constrained ($m_H < 340$ GeV) when the value of $\sin \alpha$ departs from $2v_t/v_d$. As we will discuss below, even in the region $\sin \alpha \approx 2v_t/v_d$ we can obtain lower bounds on masses that are competitive with the direct experimental bounds.

Much attention has been received by the doubly charged scalars because of the possibility of detecting them in the same sign dilepton channel. In this article, we have shown that unitarity and T -parameter impart a degeneracy among the nonstandard scalars for $v_t \lesssim 1$ GeV. Because of this, the doubly charged scalar can now decay into mainly three channels [18] – (i) same sign dileptons, (ii) a pair of same sign W -bosons and (iii) a W -boson and a singly charged scalar. As we will explain shortly, continuation of the agreement of the diphoton signal strength with the corresponding SM expectation will result in tightening the degree of degeneracy between the nonstandard scalar masses. In that case, for the usual type II scenario, the decay mode $\delta^{\pm\pm} \rightarrow W^\pm H^\pm$ is likely to be suppressed and the doubly charged scalar will decay almost exclusively into same sign dileptons and/or same sign W -bosons. When δ^{++} decays completely into two same sign dileptons, it is easy to look for it in the experiments and the bound on its mass is quite strong ($m_{++} \gtrsim 400$ GeV) [43]. In the type II seesaw model, the dominant decay mode of δ^{++} depends on the VEV of the triplet [44–47]. For $v_t \lesssim \mathcal{O}(10^{-4})$ GeV, the doubly charged scalar decays entirely into a pair of leptons and the bound from direct searches applies. But in the region $\mathcal{O}(10^{-4}) \lesssim v_t \lesssim \mathcal{O}(1)$ GeV, the δ^{++} decays mainly into a pair of W -bosons and therefore, it is very difficult to search for. In this case, a very weak bound has been placed on the mass of the doubly charged scalar using the LHC data [48–50]. In this context, we note that too low values for the masses of the charged scalar may give substantial contribution to the diphoton decay amplitude and therefore, it might be possible to set a lower bound on the masses from the observed value of the diphoton signal strength. Since all the nonstandard scalar masses are correlated, this bound can be translated into bounds on other scalar masses also. Taking into account the experimental bound from LEP-2, $m_{++} > 100$ GeV [51], along with the mass relations of Eqs. (19) and (20) we plot the 2σ allowed region from T -parameter and the observed diphoton

signal strength in Fig. 5. Although we have displayed our results for $v_t = 1$ GeV, the plot remains essentially the same for any value of $v_t \lesssim 1$ GeV. From Fig. 5, we read the following lower bounds on the nonstandard scalar masses: $m_+ \gtrsim 130$ GeV, $m_H \approx m_A \gtrsim 150$ GeV. In particular, for $v_t \lesssim \mathcal{O}(10^{-4})$ GeV when $m_{++} > 400$ GeV applies, we can give the following lower bounds on the other nonstandard scalar masses: $m_+ \gtrsim 365$ GeV, $m_H \approx m_A \gtrsim 330$ GeV. From Eqs. (38a) and (38b) we see that a more precise measurement of $\mu_{\gamma\gamma}$ has the potential to constrain the mass splittings more strongly than the T -parameter. To illustrate this point, in Fig. 5, we have also showed the futuristic projection of the 2σ allowed parameter region (in green) assuming that the diphoton signal strength will be measured to be consistent with the SM within 5% accuracy level. In that case, the bounds for $v_t \lesssim \mathcal{O}(10^{-4})$ GeV can be improved to $m_+ \gtrsim 390$ GeV, $m_H \approx m_A \gtrsim 375$ GeV.

5 Conclusions

In this paper we have revisited the constraints on the scalar sector of the type II seesaw model. We have worked under the assumption that the lightest CP-even scalar (h) has been observed the LHC. Although we have exemplified our results for $v_t = 1$ GeV, our conclusions are mostly generic and valid for any v_t of $\mathcal{O}(1$ GeV) or less. To begin with, we have re-derived the correlations between the nonstandard masses using unitarity. We have expressed all our results in terms of physical masses and mixing angles. Consequently, we have noticed that $\sin\alpha$ becomes restricted within a narrow range around $2v_t/v$ just from unitarity, whenever the neutral nonstandard scalar is heavier than 300 GeV. Moreover, for nonzero v_t , we have argued how a thin strip around $\sin\alpha = 0$ can be ruled out from $h \rightarrow \gamma\gamma$, which shrinks further the allowed band for $\sin\alpha$ (around $2v_t/v$). Using the mass relations in conjunction with the T -parameter, the separation between the masses, $|m_+ - m_{++}| \approx |m_+ - m_A|$, can be restricted to be less than 50 GeV. We have also found that, for $m_{++} > 700$ GeV, an enhancement in $\mu_{\gamma\gamma}$ is hardly possible. Finally, using the experimental range of $\mu_{\gamma\gamma}$ and T -parameter we plotted the 2σ allowed region in the m_H - m_+ plane for $\sin\alpha = 2v_t/v$. Using $m_{++} > 100$ GeV from LEP-2, we obtain the following limits on the other masses:

$$m_+ > 130 \text{ GeV}, \quad m_{H,A} > 150 \text{ GeV}.$$

Moreover, when $v_t < 10^{-4}$ GeV, the direct search bound from LHC, $m_{++} > 400$ GeV applies and then we can improve the bounds on other masses as follows:

$$m_+ > 365 \text{ GeV}, \quad m_{H,A} > 330 \text{ GeV}.$$

Remembering that T -parameter restricts the mass splitting, we may conclude that the spectrum can be determined by essentially one mass parameter for $v_t < 10^{-4}$ GeV. We have also hinted how, in future, $\mu_{\gamma\gamma}$ can play a very important role in restricting the splittings between nonstandard masses.

Acknowledgements

We thank Ipsita Saha for useful discussions. This work has been partially supported by the Spanish MINECO under grants FPA2011-23897, FPA2014-54459-P, by the ‘‘Centro de Excelencia Severo Ochoa’’ Programme under grant SEV-2014-0398 and by the ‘‘Generalitat Valenciana’’ grant GVPROMETEOII2014-087.

References

- [1] P. Minkowski, $\mu \rightarrow e\gamma$ at a Rate of One Out of 10^9 Muon Decays?, *Phys. Lett.* **B67** (1977) 421–428.
- [2] P. Ramond, *The Family Group in Grand Unified Theories*, in *International Symposium on Fundamentals of Quantum Theory and Quantum Field Theory Palm Coast, Florida, February 25-March 2, 1979*, pp. 265–280, 1979. [hep-ph/9809459](https://arxiv.org/abs/hep-ph/9809459).

- [3] M. Gell-Mann, P. Ramond and R. Slansky, *Complex Spinors and Unified Theories*, *Conf. Proc.* **C790927** (1979) 315–321, [[1306.4669](#)].
- [4] T. Yanagida, *HORIZONTAL SYMMETRY AND MASSES OF NEUTRINOS*, *Conf. Proc.* **C7902131** (1979) 95–99.
- [5] R. N. Mohapatra and G. Senjanovic, *Neutrino Mass and Spontaneous Parity Violation*, *Phys. Rev. Lett.* **44** (1980) 912.
- [6] R. Foot, H. Lew, X. G. He and G. C. Joshi, *Seesaw Neutrino Masses Induced by a Triplet of Leptons*, *Z. Phys.* **C44** (1989) 441.
- [7] E. Ma and D. P. Roy, *Heavy triplet leptons and new gauge boson*, *Nucl. Phys.* **B644** (2002) 290–302, [[hep-ph/0206150](#)].
- [8] W. Konetschny and W. Kummer, *Nonconservation of Total Lepton Number with Scalar Bosons*, *Phys. Lett.* **B70** (1977) 433.
- [9] T. P. Cheng and L.-F. Li, *Neutrino Masses, Mixings and Oscillations in $SU(2) \times U(1)$ Models of Electroweak Interactions*, *Phys. Rev.* **D22** (1980) 2860.
- [10] G. Lazarides, Q. Shafi and C. Wetterich, *Proton Lifetime and Fermion Masses in an $SO(10)$ Model*, *Nucl. Phys.* **B181** (1981) 287–300.
- [11] M. Magg and C. Wetterich, *Neutrino Mass Problem and Gauge Hierarchy*, *Phys. Lett.* **B94** (1980) 61.
- [12] J. Schechter and J. W. F. Valle, *Neutrino Masses in $SU(2) \times U(1)$ Theories*, *Phys. Rev.* **D22** (1980) 2227.
- [13] G. B. Gelmini and M. Roncadelli, *Left-Handed Neutrino Mass Scale and Spontaneously Broken Lepton Number*, *Phys. Lett.* **B99** (1981) 411.
- [14] H. M. Georgi, S. L. Glashow and S. Nussinov, *Unconventional Model of Neutrino Masses*, *Nucl. Phys.* **B193** (1981) 297.
- [15] F. Cuyppers and S. Davidson, *Bileptons: Present limits and future prospects*, *Eur. Phys. J.* **C2** (1998) 503–528, [[hep-ph/9609487](#)].
- [16] F. del Aguila and J. A. Aguilar-Saavedra, *Distinguishing seesaw models at LHC with multi-lepton signals*, *Nucl. Phys.* **B813** (2009) 22–90, [[0808.2468](#)].
- [17] P. Fileviez Perez, T. Han, G.-y. Huang, T. Li and K. Wang, *Neutrino Masses and the CERN LHC: Testing Type II Seesaw*, *Phys. Rev.* **D78** (2008) 015018, [[0805.3536](#)].
- [18] A. Melfo, M. Nemevsek, F. Nesti, G. Senjanovic and Y. Zhang, *Type II Seesaw at LHC: The Roadmap*, *Phys. Rev.* **D85** (2012) 055018, [[1108.4416](#)].
- [19] E. J. Chun and P. Sharma, *Same-Sign Tetra-Leptons from Type II Seesaw*, *JHEP* **08** (2012) 162, [[1206.6278](#)].
- [20] F. del Aguila and M. Chala, *LHC bounds on Lepton Number Violation mediated by doubly and singly-charged scalars*, *JHEP* **03** (2014) 027, [[1311.1510](#)].
- [21] E. J. Chun and P. Sharma, *Search for a doubly-charged boson in four lepton final states in type II seesaw*, *Phys. Lett.* **B728** (2014) 256–261, [[1309.6888](#)].
- [22] F. del Aguila, M. Chala, A. Santamaria and J. Wudka, *Discriminating between lepton number violating scalars using events with four and three charged leptons at the LHC*, *Phys. Lett.* **B725** (2013) 310–315, [[1305.3904](#)].
- [23] G. K. Leontaris, K. Tamvakis and J. D. Vergados, *Lepton and Family Number Violation From Exotic Scalars*, *Phys. Lett.* **B162** (1985) 153–159.

- [24] A. Pich, A. Santamaria and J. Bernabeu, $\mu \rightarrow e\gamma$ decay in the Scalar Triplet Model, *Phys. Lett.* **B148** (1984) 229–233.
- [25] J. Bernabeu and A. Santamaria, Lepton Flavor Violating Decay of the Z^0 in the Scalar Triplet Model, *Phys. Lett.* **B197** (1987) 418.
- [26] S. M. Bilenky and S. T. Petcov, *Massive Neutrinos and Neutrino Oscillations*, *Rev. Mod. Phys.* **59** (1987) 671.
- [27] A. G. Akeroyd, M. Aoki and H. Sugiyama, Lepton Flavour Violating Decays $\tau \rightarrow \bar{\nu}_\tau \text{ anti-}l \text{ } ll$ and $\mu \rightarrow \bar{\nu}_\tau \text{ } e \text{ } \gamma$ in the Higgs Triplet Model, *Phys. Rev.* **D79** (2009) 113010, [0904.3640].
- [28] A. Arhrib, R. Benbrik, M. Chabab, G. Moulataka, M. C. Peyranere, L. Rahili et al., The Higgs Potential in the Type II Seesaw Model, *Phys. Rev.* **D84** (2011) 095005, [1105.1925].
- [29] E. J. Chun, H. M. Lee and P. Sharma, Vacuum Stability, Perturbativity, EWPD and Higgs-to-diphoton rate in Type II Seesaw Models, *JHEP* **11** (2012) 106, [1209.1303].
- [30] F. Arbabifar, S. Bahrami and M. Frank, Neutral Higgs Bosons in the Higgs Triplet Model with nontrivial mixing, *Phys. Rev.* **D87** (2013) 015020, [1211.6797].
- [31] P. S. Bhupal Dev, D. K. Ghosh, N. Okada and I. Saha, 125 GeV Higgs Boson and the Type-II Seesaw Model, *JHEP* **03** (2013) 150, [1301.3453].
- [32] J. F. Gunion, R. Vega and J. Wudka, Higgs triplets in the standard model, *Phys. Rev.* **D42** (1990) 1673–1691.
- [33] P. Dey, A. Kundu and B. Mukhopadhyaya, Some consequences of a Higgs triplet, *J. Phys.* **G36** (2009) 025002, [0802.2510].
- [34] S. Kanemura and K. Yagyu, Radiative corrections to electroweak parameters in the Higgs triplet model and implication with the recent Higgs boson searches, *Phys. Rev.* **D85** (2012) 115009, [1201.6287].
- [35] C. Bonilla, R. M. Fonseca and J. W. F. Valle, Consistency of the triplet seesaw model revisited, *Phys. Rev.* **D92** (2015) 075028, [1508.02323].
- [36] L. Lavoura and L.-F. Li, Making the small oblique parameters large, *Phys. Rev.* **D49** (1994) 1409–1416, [hep-ph/9309262].
- [37] PARTICLE DATA GROUP collaboration, K. A. Olive et al., Review of Particle Physics, *Chin. Phys.* **C38** (2014) 090001.
- [38] THE ATLAS AND CMS collaboration, Measurements of the Higgs boson production and decay rates and constraints on its couplings from a combined ATLAS and CMS analysis of the LHC pp collision data at $\sqrt{s} = 7$ and 8 TeV, *ATLAS-CONF-2015-044* (2015) .
- [39] J. F. Gunion, H. E. Haber, G. L. Kane and S. Dawson, *The Higgs Hunter’s Guide*, *Front. Phys.* **80** (2000) 1–448.
- [40] C.-S. Chen, C.-Q. Geng, D. Huang and L.-H. Tsai, $h \rightarrow Z\gamma$ in Type-II seesaw neutrino model, *Phys. Lett.* **B723** (2013) 156–160, [1302.0502].
- [41] N. Haba, H. Ishida, N. Okada and Y. Yamaguchi, Vacuum stability and naturalness in type-II seesaw, *Eur. Phys. J.* **C76** (2016) 333, [1601.05217].
- [42] G. Bhattacharyya and D. Das, Nondecoupling of charged scalars in Higgs decay to two photons and symmetries of the scalar potential, *Phys. Rev.* **D91** (2015) 015005, [1408.6133].
- [43] CMS collaboration, Search for a doubly-charged Higgs boson with $\sqrt{s} = 8$ TeV pp collisions at the CMS experiment, *CMS-PAS-HIG-14-039* (2016) .

- [44] T. Han, B. Mukhopadhyaya, Z. Si and K. Wang, *Pair production of doubly-charged scalars: Neutrino mass constraints and signals at the LHC*, *Phys. Rev.* **D76** (2007) 075013, [[0706.0441](#)].
- [45] J. Garayoa and T. Schwetz, *Neutrino mass hierarchy and Majorana CP phases within the Higgs triplet model at the LHC*, *JHEP* **03** (2008) 009, [[0712.1453](#)].
- [46] M. Kadastik, M. Raidal and L. Rebane, *Direct determination of neutrino mass parameters at future colliders*, *Phys. Rev.* **D77** (2008) 115023, [[0712.3912](#)].
- [47] A. G. Akeroyd, M. Aoki and H. Sugiyama, *Probing Majorana Phases and Neutrino Mass Spectrum in the Higgs Triplet Model at the CERN LHC*, *Phys. Rev.* **D77** (2008) 075010, [[0712.4019](#)].
- [48] S. Kanemura, K. Yagyu and H. Yokoya, *First constraint on the mass of doubly-charged Higgs bosons in the same-sign diboson decay scenario at the LHC*, *Phys. Lett.* **B726** (2013) 316–319, [[1305.2383](#)].
- [49] S. Kanemura, M. Kikuchi, H. Yokoya and K. Yagyu, *LHC Run-I constraint on the mass of doubly charged Higgs bosons in the same-sign diboson decay scenario*, *PTEP* **2015** (2015) 051B02, [[1412.7603](#)].
- [50] Z. Kang, J. Li, T. Li, Y. Liu and G.-Z. Ning, *Light Doubly Charged Higgs Boson via the WW^* Channel at LHC*, *Eur. Phys. J.* **C75** (2015) 574, [[1404.5207](#)].
- [51] DELPHI collaboration, J. Abdallah et al., *Search for doubly charged Higgs bosons at LEP-2*, *Phys. Lett.* **B552** (2003) 127–137, [[hep-ex/0303026](#)].